

Accepted Manuscript

Structure-based design, synthesis and biological evaluation of a newer series of pyrazolo[1,5-*a*]pyrimidine analogues as potential anti-tubercular agents

Palmi Modi, Shivani Patel, Mahesh Chhabria

PII: S0045-2068(18)31401-9
DOI: <https://doi.org/10.1016/j.bioorg.2019.02.044>
Reference: YBIOO 2819

To appear in: *Bioorganic Chemistry*

Received Date: 1 December 2018
Revised Date: 23 January 2019
Accepted Date: 20 February 2019

Please cite this article as: P. Modi, S. Patel, M. Chhabria, Structure-based design, synthesis and biological evaluation of a newer series of pyrazolo[1,5-*a*]pyrimidine analogues as potential anti-tubercular agents, *Bioorganic Chemistry* (2019), doi: <https://doi.org/10.1016/j.bioorg.2019.02.044>

This is a PDF file of an unedited manuscript that has been accepted for publication. As a service to our customers we are providing this early version of the manuscript. The manuscript will undergo copyediting, typesetting, and review of the resulting proof before it is published in its final form. Please note that during the production process errors may be discovered which could affect the content, and all legal disclaimers that apply to the journal pertain.



Structure-based design, synthesis and biological evaluation of a newer series of pyrazolo[1,5-*a*]pyrimidine analogues as potential anti-tubercular agents.

PalmiModi^{a,b,d}, ShivaniPatel^{a,c}, Mahesh Chhabria^a

^aDepartment of Pharmaceutical Chemistry, L. M. College of Pharmacy, Navrangpura, Ahmedabad – 380009 (Gujarat), India

^bDepartment of Pharmacy, Dharmsinh Desai University, Nadiad – 387001(Gujarat), India

^cDivision of biological and life sciences, Ahmedabad University, Ahmedabad – 380009(Gujarat), India

^dDepartment of Pharmaceutical Chemistry, L. J. Institute of Pharmacy, Ahmedabad-382210 (Gujarat), India.

Corresponding author

✉ Mahesh T. Chhabria

E-mail address- mahesh.chhabria@rediffmail.com

Abstract:

In-depth study of structure-based drug designing can provide vital leads for the development of novel, clinically active molecules. In this present study, twenty six novel pyrazolo[1,5-*a*]pyrimidine analogues (6a-6z) were designed using molecular docking studies. The designed molecules were synthesized in good yields. Structural elucidation of the synthesized molecules was carried out using IR, MS, ¹H-NMR and ¹³C-NMR spectroscopy. All the synthesized compounds were evaluated for their *in-vitro* anti-tubercular activity against H37Rv strain by Alamar Blue assay method. Most of the synthesized compounds displayed potent anti-tubercular activities. Amongst all the tested compounds **6p,6g, 6n** and **6h** exhibited promising anti-tubercular activity. Further, these potent compounds were gauged for MDR-TB, XDR-TB and cytotoxic study. None of these compounds exhibited potent cytotoxicity. Stability of protein ligand complex was further evaluated by molecular dynamics simulation for 10ns. All these results indicate that the synthesized compounds could be potential leads for further development of new potent anti-tubercular agents.

Key words: *Mycobacterium tuberculosis*; molecular docking; Molecular dynamics; Pyrazolo[1,5-*a*]pyrimidine hybrids

1. Introduction

Tuberculosis is the life-threatening infectious disease caused by the bacterium, *Mycobacterium tuberculosis* [1]. In addition to this MDR-TB and XDR-TB associated with HIV is one of the continual diseases with its widespread characteristic [2]. Approximately 13 million people need to be treated by the year 2020. The biggest challenge in management of tuberculosis treatment is the hostility of the mycobacterial infection [3]. To overcome this increased resistance new class of anti-tubercular agents acting through novel mechanism of action are one of the urgent requirement to combat *M. tuberculosis* infections. Mycolic acid is the central constituent of causative pathogen. Most of the currently available anti-tubercular drugs act through inhibition of the mycolic acid synthesis, which is the long chain fatty acid of 60-90 carbons with α -alkyl β -hydroxy groups [4, 5]. InhA (enoyl acyl reductase enzyme) is the major targeted enzyme involved in the fatty acid biosynthesis pathway of *Mycobacterium tuberculosis* [6]. It is one of the emerging targets for the development of novel anti-tubercular agents [7].

Heterocyclic derivatives have extensive range of biological importance and applications. Individual pyrazole and pyrimidine nucleus are the nitrogen containing heterocyclic molecules which constitute the largest portion of medicinal important moieties [8, 9]. They exhibits a wide spectrum of biological activities including adenosine receptor antagonists [10], anti-schistosomal, anti-trypanosomal and sedative [11], anxiolytic [12], HMG-CoA reductase inhibitors [13], KDR kinase inhibitors [14], COX-1, selective COX-2 inhibitors [15], kinase inhibitors [16], HIV reverse transcriptase inhibitors [17], anti-malarial and antifungal [18] and many more. The lipophilicity of these chemophores plays an important role in their physicochemical properties and biological activity.

Inspired by the activities of these potent motifs, computational methods were applied to incorporate these two individual pharmacophores in a single framework as pyrazolo[1,5-*a*]pyrimidine hybrid analogues. These condensed hetrocyclic derivatives are known to act as potential anti-tubercular agents by inhibiting FAB-I enzyme involved in the fatty acid synthesis of the mycobacterium cell wall [19]. The current work describes the synthesis of novel pyrazolo[1,5-*a*]pyrimidine hybrid analogues with encouraging anti-mycobacterial activity against *M. tuberculosis* H37Rv strain.

In the present study, molecular docking technique was applied on enoyl acyl reductase protein enzyme (PDB: 2H7M) to identify the important interactions and predict potent hit molecules [20]. We have designed a new class of pyrazolo[1,5-*a*]pyrimidine hybrids to improve the anti-tubercular activity especially against the drug resistance *M.*

tuberculosis stain. Also the designed compounds were further filtered through ADMET properties to check drug likeliness of predicted molecules. All the designed molecules were synthesized and screened for their anti-tubercular activity using Alamar Blue Assay Method against H37Rv strain. Potent hit molecules from preliminary screening were further opted for MDR-TB, XDR-TB and cytotoxicity on mammalian VERO cell line [20]. Based on the biological activities the most potent compound was subjected to molecular dynamics simulation to check its stability with respect to the protein structure.

2. Results and Discussion

2.1. Chemistry

The route of synthesis for the final derivatives of 7-hydroxy-5-methyl-N-substituted phenyl-2-(substituted phenylamino)pyrazolo[1,5-a]pyrimidine-3-carboxamide (**6a-6z**) has been summarised in **scheme 1**. First step involves the synthesis of 2-cyano-N-(substitutedphenyl)acetamide(**2a-2o**) derivatives by nucleophilic addition reaction between ethyl cyanoacetate(**1**) and substituted anilines. Further, in presence of base and carbon disulphide it undergoes for nucleophilic addition reaction on active methylene of 2-cyano-N-(substitutedphenyl)acetamide(**2a-2o**) followed by methylation with dimethyl sulphate, yields S, S acetal(**3a-3o**). These S, S acetal(**3a-3o**) derivatives further undergo for nucleophilic substitution reaction by addition of substituted anilines and cyclic aliphatic amines for the formation of Keten S, N- acetals(**4a-4z**). Due to presence of electrophilic and nucleophilic centres these Keten S, N- acetal possesses high reactivity and that can be utilised in regioselective ring closure strategies with hydrazine hydrate for the formation of 5-amino-N-substituted phenyl-3-(substituted phenylamino)-1H-pyrazole-4-carboxamide (**5a-5z**). Pyrazole derivatives, (**5a-5z**) on cyclocondensation with ethyl aceto acetate give the targeted compound 7-hydroxy-5-methyl-N-substituted phenyl-2-(substituted phenylamino)pyrazolo[1,5-a]pyrimidine-3-carboxamide (**6a-6z**). All the synthesised compounds (**6a-6z**) characterized by IR, MS, ¹H-NMR, ¹³C-NMR spectroscopy after purification. Spectrum values of all the synthesized compounds are presented in the experimental part.

2.2. In-silico molecular docking approach

Molecular docking is a structure based drug design approach which is an essential part of the drug discovery assigning knowledge of enzyme-inhibitor complex with respect to the binding affinity and binding mode. Here we have used Glide module of Schrodinger software (Maestro v10.1, Schrodinger, LLC, NEW YORK, NY) for carrying out docking studies. The predicted New Chemical Entities (**6a-6z**) followed by the Lipinski's rule of five were docked

into the active site of InhA enzyme (PDB ID: 2H7M) retrieved from the protein data bank (He et al. 2007). The co-crystalline structure 1-cyclohexyl-*N*-(3,5-dichlorophenyl)-5-oxopyrrolidine-3-carboxamide derivative possess -8.17 docking score with Ile21, Met103, Met147, Phe149, Pro156, Tyr158, Lys165, Ile 202 and Leu218 interacting aminoacid residues. The MIC values and docking score of the NCE's were dealing with the numbers. So we have selected some of the most potent inhibitors **6g**, **6h**, **6n** and **6p** which possess -8.23, -7.27 and -8.89 and -9.23 docking scores respectively and discussed them in detail below.

All the NCE's anchors same co-ordinates in the substrate binding loop Gly 96, Met 147, Phe149, Pro 156, Tyr 158, Met161, Lys 165, Ala198, Met199, Ile202 and Val203 as observed for the native ligand. Compound [2-((*p*-Chlorophenyl)amino)-7-hydroxy-5-methyl-*N*-(*p*-tolyl)pyrazolo[1,5-*a*]pyrimidine-3-carboxamide(**6g**)] **Figure 1(a)** showed π - π interaction of its phenyl ring with Lys165 and hydrophobic interactions with Ile21, Met103, Met147, Phe149, Pro156, Tyr158, Ile 202 and Leu218. Pyrazolo[1,5-*a*]pyrimidine moiety was occupied because of the hydrophobic interaction with Ile21, Met147, Phe149, Lys165, Gly192 and Pro193. The compound [7-Hydroxy-*N*-(*o*-methoxyphenyl)-5-methyl-2-(*m*-tolylamino)pyrazolo[1,5-*a*]pyrimidine-3-carboxamide (**6n**)] **Figure 1(b)** having hydrogen bond interactions with Ile194 and shows that the major important hydrophobic interacting residues are Ile21, Met103, Met147, Phe149, Pro156, Tyr158, Lys 165, Ile 194, Leu218, and Ile202. Compounds 2-((3,4-difluorophenyl)amino)-*N*-(*p*-fluorophenyl)-7-hydroxy-5-methylpyrazolo[1,5-*a*]pyrimidine-3-carboxamide (**6p**) **Figure 1(c)** and 2-((3,4-dichlorophenyl)amino)-7-hydroxy-5-methylpyrazolo[1,5-*a*]pyrimidine-3-carboxamide (**6h**) **Figure 1(d)** have molecular interactions with Ile194, and hydrophobic interaction with Ile21, Met147, Phe149, Tyr158, Lys 165, Leu218, Pro156, Met103, Ile202 indicating similar interaction as the co-crystalline structure which can be novel *M. tuberculosis* inhibitor. These findings suggest that the newly designed compounds may be considered as potential scaffolds for anti-tubercular drug discovery.

2.3. *In-silico* ADME prediction

Satisfactory ADMET profile with good effectiveness is one of the major benchmark for the completion of a drug. Obtained potential leads of Pyrazolo[1,5-*a*]pyrimidine derivatives based on molecular docking study and anti-tubercular potential (**6a-6z**) were further opted for *in-silico* ADMET prediction to check its druggability using QikProp module in Schrodinger. The results are shown in **Table 1**.

2.4. Biological Evaluation

2.4.1. Anti-tubercular studies

Anti-tubercular potential was performed using MicroplateAlamar Blue Assay (MABA) method for the preliminary screening of the newly synthesized targeted compounds against *Mycobacterium tuberculosis* H37Rv strain (Cho et al. 2015). Some of the finally synthesized pyrazolo[1,5-*a*]pyrimidine derivatives retains reasonable inhibitory activity compared with the standard drugs Ciprofloxacin, Pyrazinamide and Streptomycin. The results of the *in-vitro* anti-tubercular activity of the title compounds (**6a–6z**) in MIC levels have shown in **Table 2**. Amongst screened all the final molecules, **6p** with electron withdrawing substitutions on both side of the aryl ring yields excellent activity against *M. tuberculosis* H₃₇Rv strain with MIC value 0.8 µg/mL. This obtained result found to be more potent that the compared all the standard drugs. Compounds **6g** and **6n** have shown MIC of 3.12 µg/mL which are comparable to the standard drugs Ciprofloxacin and Pyrazinamide. One of the compound **6h** showed MIC of 6.25 mg/mL which is comparable to the standard drug streptomycin. However with electron donating substitutions **6a**, **6b**, **6w** and **6y** starts to loss potency with MIC of 12.5 µg/mL. Remaining other molecules **6e**, **6s** and **6x** possess anti-tubercular activity with MIC of 25 µg/mL, while **6c**, **6d**, **6f**, **6i-6m**, **6o**, **6q**, **6r**, **6t**, **6v** and **6z** have MIC of 50 µg/mL each. Compound **6u** exhibited MIC of 100 µg/mL. In view of good anti-tubercular activity of compounds **6g**, **6h**, **6n** and **6p** were further evaluated for their MDR-TB, XDR-TB and *in vitro* cytotoxicity study using Vero cell line.

2.4.2. Structure Activity Relationship (SAR)

The whole structure activity relationship has been summarised in **Figure 2**. A good anti-TB activity may be attributed to the presence of electron withdrawing substitutions at R or R' or at both the aryl rings attached to pyrazolo[1,5-*a*]pyrimidine. Similarly, replacement of electron donating substituents at one or both of the phenyl rings attenuated the anti-tubercular activity. Here Heteroaromatic rings like N-ethyl piperazine, Pyrrolidine and Morpholine at R' position were found to have decrease the potency.

2.4.3. MDR-TB and XDR-TB

On the basis of anti-tubercular activity, Lowenstein-Jensen medium (L.J. medium) method was used for the compound **6g**, **6h**, **6n** and **6p** to check its vulnerability towards multidrug resistant Tb (MRD-TB) and extensively drug-resistant TB (XDR-TB). The results are summarized in **Table 3**.

2.4.4. Cytotoxicity assay

Selected potent molecules **6g**, **6h**, **6n** and **6p** based on anti-tubercular activity were further evaluated for its cytotoxic activity against a mammalian Vero cell line using 3-(4,5-dimethylthiazo-2-yl)-2,5-diphenyl-tetrazolium bromide (MTT) assay. Here isoniazid was

used as a positive control (Maria et al. 2017). The result of study summarised in **Table 3**. Compounds **6g** had 20.99 $\mu\text{g/mL}$ of IC_{50} , whereas compounds **6h** and **6n** shows weaker effect on cancer cell line with IC_{50} value of 29.02 $\mu\text{g/mL}$ and 21.2 $\mu\text{g/mL}$ respectively. However, compound **6p** has the lowest sensitivity with IC_{50} of 13.57 $\mu\text{g/mL}$. The resulted active molecules found relatively non-toxic against mammalian Vero cell line. So, it could be inferred that the presence of electron-withdrawing substitutions on the phenyl ring increase the cytotoxicity potential of the pyrazolo[1,5-*a*]pyrimidine.

2.5. Molecular dynamic simulations

The protein-ligand complex was further subjected to MD simulation after demonstrating significant docking interactions. The stability of simulated system was analysed through RMSD and RMSF values with respect to the unbound protein structure (John et al. 2015; Schuttelkopf et al. 2004). The temporal RMSD plot of co-crystalline and **6p** complex is shown in **Figure 3(a)**. The curve exhibited minor fluctuation of 2.0 Å, which demonstrates the stability of the ligand within the binding pocket. Further, the RMSF plot of complex revealed that most of the residues fluctuate below 2.5 Å and few residues show fluctuation up to 4.5 Å **Figure 3(b)** (Martyna et al. 1994). High fluctuations were observed in *N*- and *C* terminal region compared to any other part of protein. Subsequently, the favourable contacts between the protein residues and ligand atoms were found with Tyr 158, Lys 165, Ile 194, Met 199 and Ile 202 conserved for MD stimulation which has been displayed in **Figure 4**. The H-bonding interactions were formed with Lys 165 and Tyr 196 and Ile 194 through water molecule which contributed to the binding affinity of the ligand. These essential residual interactions with **6p** supported its inhibitory potency as anti-tubercular agent.

3. Conclusion

In the present work we have designed and synthesized newer series of 7-hydroxy-5-methyl-*N*-substitutedphenyl-2-(substitutedphenylamino)pyrazolo[1,5-*a*]pyrimidine-3-carboxamide (6a-6z) derivatives in which pyrazole and pyrimidine both the heterocyclic rings were fused. Activity of synthesized final potent derivatives **6g**, **6h**, **6n** and **6p** possess potent anti-tuberculosis activities compared to the reference standards drugs. Molecular modelling and docking studies also suggested that compounds **6g**, **6h**, **6n** and **6p** interacted with InhA enzyme more efficiently. So, it is concluded that compounds with electron withdrawing substituents increases the potency. Further this powerful supposition opens up the discovery of newer potential targeted molecules as novel anti-tuberculosis agents.

4. Experimental

4.1. Chemistry

Chemicals and solvents of laboratory grade were purchased from commercially available suppliers Rankem India Ltd., Loba, Sigma Aldrich and SpecrochemPvt. Ltd and used after purification. Melting points of synthesized final compounds were determined by open capillary method using VMP-D (VEEGO) model and are uncorrected. Completion of the reaction was monitored by iodine vapours, UV radiations and precoated thin layer chromatography sheets (Merck60 F254, 0.25 mm). The Infrared (IR) spectra for final compounds were recorded in KBr using FT-IR 8400S Shimadzu Fourier Transform spectrophotometer. Mass spectra were taken using Perkin-Elmer LC-MS PE Sciex API/65. Bruker AVANCE-II 400 MHz spectrophotometer was used to take ^1H NMR spectra and ^{13}C NMR. Chemical shifts are expressed as parts per million (ppm), peak patterns were used to describe as: s (singlet), d (doublet), t (triplet), q (quartet) or m (multiplet). Tetramethylsilane (TMS) was used as an internal standard and DMSO- d_6 as solvent.

4.1.1. Preparation 2-cyano-N-(substituted phenyl)acetamide (2)

To a round bottom flask ethyl cyanoacetate (0.0468 mol) and substituted anilines(0.0468 mol) was added. The reaction was refluxed for 8 hours using 15 mL DMF as a solvent. Precoated TLC was used to confirm the completion of the reaction. After completion, the reaction was poured into ice-cold water to obtain crude solid. Further to yield pure crystalline product obtained crude solid was filtered, dried and recrystallized from ethanol.

4.1.2. Preparation of 2-cyano-N-(substituted phenyl)-3,3bis(methylthio)acrylamide (3)

2-cyano-N-(substituted phenyl)acetamide (0.00523 mol) was added to the solution of potassium hydroxide (0.01046mol) containing 5 ml of water at cooled temperature of 0-5°C with continuous stirring. To that carbon disulphide (0.00523mol) was added drop wise followed by 15 ml of dimethyl formamide (DMF). Further dimethylsulphate (0.01046 mol) was added drop wise followed by 2 hours of stirring. After completion of stirring pour the reaction into ice-cold mixture to obtain the solid. The solid was filtered, washed with water and recrystallized from methanol to obtain colorless crystalline product [21].

4.1.3. Preparation of 2-cyano-3-(methylthio)-N-substituted phenyl-3-(substituted phenylamino)acrylamide (4)

Differently synthesized 2-cyano-N-(substituted phenyl)-3,3bis(methylthio)acrylamide (0.003 mol) and substituted aniline (0.003 mol) was dissolved in 10 ml isopropyl alcohol (IPA) followed by reflux for 14-15 hours. Completion of the reaction was monitored by TLC. After that the reaction mixture was quenched into ice cold water to obtain dried filtered solid. Further dried solid was recrystallization from IPA to yielded crystalline product [22].

4.1.4. Preparation of 5-amino-N-substituted phenyl-3-(substituted phenylamino)-1H-pyrazole-4-carboxamide (5)

Above synthesized 2-cyano-3-(methylthio)-N-substituted phenyl-3-(substituted phenylamino)acrylamide (0.0104 mol) and hydrazine hydrate (0.0104 mol) was refluxed for 3-4 hours with 20 ml ethanol in a round bottom flask. Completion of the reaction was monitored by TLC. After completion of the reaction, ethanol was distilled off and obtained recrystallized solid was filtered and dried [23].

4.1.5. General procedure for the synthesis of 7-hydroxy-5-methyl-N-substituted phenyl-2-(substituted phenylamino)pyrazolo[1,5-a]pyrimidine-3-carboxamide (6a-6z)

Mixture of ethyl aceto acetate (0.01029 mol) and 5-amino-N-substituted phenyl-3-(substituted phenylamino)-1H-pyrazole-4-carboxamide (0.001029 mol) was refluxed in an oil bath for 1-2 hours. The solid product was separated out from the reaction mixture indicates the completion of the reaction. The obtained was filtered and recrystallized using chloroform to obtain pure crystalline product.

4.1.5.1. 7-Hydroxy-N-(4-methoxyphenyl)-2-((4-methoxyphenyl)amino)-5-methylpyrazolo[1,5-a]pyrimidine-3-carboxamide (6a)

White solid; Yield: 80%; M.P. 276-278°C; IR (KBr, cm^{-1}) 3455 (-OH), 3323 (-NH str.), 1666 (-CO-NH str.), 1240 (C-N str.), 1033 (C-O-C); ^1H NMR (400 MHz, DMSO- d_6 , δ , ppm): δ 11.89 (s, 1H, OH-Pyrimidine, D_2O exchangeable), δ 9.56 (s, 1H, CONH-Ar., D_2O exchangeable), δ 8.68 (s, 1H, NH-Pyrazole, D_2O exchangeable), δ 6.88- 7.61 (m, 8H, -CH-Ar.), δ 5.75 (s, 1H, -CH-Pyrimidine), δ 3.72- 3.76 (s, 6H, - OCH_3 -Ar.), δ 2.35 (s, 3H, - CH_3 -Pyrimidine); ^{13}C NMR (400 MHz, DMSO- d_6 , δ , ppm): 161.22, 155.57, 154.82, 153.49, 153.21, 147.20, 140.30, 134.42, 131.59, 122.56, 118.60, 114.04, 113.61, 98.14, 87.33, 55.17, 55.15, 18.79; LCMS (M/Z) Calculated for $\text{C}_{22}\text{H}_{21}\text{N}_5\text{O}_4$: 419.4; Obtained MS: 420.2 (M+1)

4.1.5.2. 2-((4-Chlorophenyl)amino)-7-hydroxy-N-(4-methoxyphenyl)-5-methylpyrazolo[1,5-a]pyrimidine-3-carboxamide (6b)

White solid; Yield: 86.42%; M.P 317-320 °C; IR (KBr, cm^{-1}) 3352 (-NH str.), 1666 (-CO-NH str.), 1238 (C-N str.), 1033 (C-O-C), 825, 551 (C-Cl); ^1H NMR (400 MHz, DMSO- d_6 , δ ppm) δ 11.96 (s, 1H, OH-Pyrimidine, D_2O exchangeable), δ 9.64 (s, 1H, CONH-Ar, D_2O exchangeable), δ 8.97 (s, 1H, NH-Pyrazole, D_2O exchangeable), δ 6.93- 7.74 (m, 8H, -CH-Ar.), δ 5.78 (s, 1H, -CH-Pyrimidine), δ 3.75 (s, 3H, - OCH_3 -Ar.), δ 2.35 (s, 3H, - CH_3 -Pyrimidine); ^{13}C NMR (400 MHz, DMSO- d_6 , δ ppm): 161.22, 155.57, 154.82, 153.49, 153.21, 147.20, 140.30, 134.42, 131.59, 122.56, 118.60, 114.04, 113.61, 98.14, 87.33, 18.79;

LCMS (M/Z) Calculated for C₂₁H₁₈ClN₅O₃: 423.9; Obtained MS (M/Z): 424.2 (M+1), 426.1 (M+2)

4.1.5.3. 2-((2,3-Dimethylphenyl)amino)-7-hydroxy-N-(4-methoxyphenyl)-5-methylpyrazolo[1,5-a]pyrimidine-3-carboxamide (6c)

White solid; Yield 68.22%; M. P. 280-284 °C; IR (KBr, cm⁻¹) 3363 (-NH str.), 1656 (-CO-NH str.), 1247 (C-N str.), 1039 (C-O-C); ¹H NMR (400 MHz, DMSO-d₆, δ ppm) δ 11.98 (s, 1H, OH-Pyrimidine, D₂O exchangeable), δ 9.54 (s, 1H, CONH-Ar., D₂O exchangeable), δ 9.06 (s, 1H, NH-Pyrazole, D₂O exchangeable), δ 6.77- 8.21 (m, 8H, -CH-Ar.), δ 5.79 (s, 1H, -CH-Pyrimidine), δ 3.75 (s, 3H, -OCH₃-Ar.), δ 2.17-2.50 (m, 6H, -CH₃-Ar.); δ 2.17-2.50 (s, 3H, -CH₃-Pyrimidine); ¹³C NMR (400 MHz, DMSO-d₆, δ ppm) : 161.79, 155.70, 153.71, 138.99, 136.17, 131.38, 125.68, 122.86, 122.67, 122.56, 115.24, 113.72, 55.20, 20.47, 18.81, 12.91; LCMS (M/Z) Calculated for C₂₃H₂₃N₅O₃: 417.5; Obtained MS (M/Z): 418.3 (M+1) 419.4 (M+2)

4.1.5.4. 7-Hydroxy-N-(4-methoxyphenyl)-5-methyl-2-(phenylamino)pyrazolo[1,5-a]pyrimidine-3-carboxamide (6d)

White solid; Yield 84.24%; M. P. 320-322 °C; IR (KBr, cm⁻¹) 3384 (-NH str.), 1616 (-CO-NH str.), 1230 (C-N str.), 1035 (C-O-C); ¹H NMR (400 MHz, DMSO-d₆, δ ppm) δ 11.94 (s, 1H, OH-Pyrimidine, D₂O exchangeable), δ 9.60 (s, 1H, CONH-Ar., D₂O exchangeable), δ 8.88 (s, 1H, NH-Pyrazole, D₂O exchangeable), δ 6.89- 7.67 (m, 9H, -CH-Ar.), δ 5.77 (s, 1H, -CH-Pyrimidine), δ 3.42 (s, 3H, -OCH₃-Ar.), δ 2.50 (m, 3H, -CH₃-Pyrimidine); ¹³C NMR (400 MHz, DMSO-d₆, δ ppm) : 161.17, 155.62, 154.86, 152.88, 149.93, 140.93, 140.23, 131.52, 128.79, 122.60, 120.42, 117.05, 113.61, 98.14, 87.69, 55.18, 18.84; LCMS (M/Z) Calculated for C₂₁H₁₉N₅O₃: 389.1; Obtained MS (M/Z): 390.4 (M+1)

4.1.5.5. 7-Hydroxy-N-(4-methoxyphenyl)-5-methyl-2-morpholinopyrazolo[1,5-a]pyrimidine-3-carboxamide (6e)

White solid; Yield 48.12%; M.P. 291-295 °C; IR (KBr, cm⁻¹) 3359 (-NH str.), 1683 (-CO-NH str.), 1242 (C-N str.), 1033 (C-O-C); ¹H NMR (400 MHz, DMSO-d₆, δ ppm) : δ 11.94 (s, 1H, OH-Pyrimidine, D₂O exchangeable), δ 9.60 (s, 1H, CONH-Ar., D₂O exchangeable), δ 6.90- 7.67 (m, 12H, -CH-Ar., D₂O exchangeable), δ 5.87 (s, 1H, -CH-Pyrimidine), δ 3.42 (s, 3H, -OCH₃-Ar), δ 2.27 (m, 3H, -CH₃-Pyrimidine); ¹³C NMR (400 MHz, DMSO-d₆, δ ppm) : 159.88, 120.80, 113.83, 90.21, 65.85, 55.17, 16.51; LCMS (M/Z) Calculated for C₁₉H₂₁N₅O₄: 383.4; Obtained MS (M/Z): 384.2 (M+1)

4.1.5.6. 7-Hydroxy-5-methyl-2-(phenylamino)-N-(p-tolyl)pyrazolo[1,5-a]pyrimidine-3-carboxamide (6f)

White solid; Yield 72.89%; M. P. 283-286 °C; IR (KBr, cm^{-1}) 3377 (-NH str.), 1656 (-CO-NH str.), 1232 (C-N str.); ^1H NMR (400 MHz, DMSO- d_6 , δ ppm) : δ 11.96 (s, 1H, OH-Pyrimidine, D_2O exchangeable), δ 9.65 (s, 1H, CONH-Ar., D_2O exchangeable), δ 8.85 (s, 1H, NH-Pyrazole, D_2O exchangeable), δ 6.89- 7.67 (m, 9H, -CH-Ar.), δ 5.77 (s, 1H, -CH-Pyrimidine), δ 2.29 -2.35 (s, 3H, - CH_3 -Ar), δ 2.29 -2.35 (s, 3H, - CH_3 -Pyrimidine); ^{13}C NMR (400 MHz, DMSO- d_6 , δ ppm) : 161.29, 154.85, 152.82, 149.98, 140.96, 140.30, 136.07, 132.54, 128.86, 128.79, 120.86, 120.42, 117.06, 98.15, 87.66, 20.49, 18.85; LCMS (M/Z) Calculated for $\text{C}_{21}\text{H}_{19}\text{N}_5\text{O}_2$: 373.4; Obtained MS (M/Z): 374.2 (M+1)

4.1.5.7. 2-((4-Chlorophenyl)amino)-7-hydroxy-5-methyl-N-(p-tolyl)pyrazolo[1,5-a]pyrimidine-3-carboxamide (6g)

White solid; Yield 68.33 %; M. P. 262-264 °C; IR (KBr, cm^{-1}) 3342 (-NH str.), 1668 (-CO-NH str.), 1234 (C-N str.), 811, 663 (C-Cl); ^1H NMR (400 MHz, DMSO- d_6 , δ ppm) : δ 11.97 (s, 1H, OH-Pyrimidine, D_2O exchangeable), δ 9.67 (s, 1H, CONH-Ar., D_2O exchangeable), δ 8.95 (s, 1H, NH-Pyrazole, D_2O exchangeable), δ 7.15- 7.73 (m, 8H, -CH-Ar.), δ 5.77 (s, 1H, -CH-Pyrimidine), δ 2.23-2.47 (s, 3H, - CH_3 -Ar), δ 2.23-2.47 (s, 3H, - CH_3 -Pyrimidine); ^{13}C NMR (400 MHz, DMSO- d_6 , δ ppm) : 161.29, 154.85, 152.82, 149.98, 140.96, 140.30, 136.07, 132.54, 128.86, 128.79, 120.86, 120.42, 117.06, 98.15, 87.66, 20.49; LCMS (M/Z) Calculated for $\text{C}_{21}\text{H}_{19}\text{ClN}_5\text{O}_2$: 407.1; Obtained MS (M/Z): 408.5 (M+1)

4.1.5.8. 2-((3,4-Dichlorophenyl)amino)-7-hydroxy-5-methylpyrazolo[1,5-a]pyrimidine-3-carboxamide (6h)

Yellow solid; Yield 54.43%; M. P. 308-310 °C; IR (KBr, cm^{-1}) 3325, 3238 (-N-H str.), 1658 (-CO-N-H str.), 1247 (C-N str.), 850, 698 (C-Cl); ^1H NMR (400 MHz, DMSO- d_6 , δ ppm) : δ 11.60 (s, 1H, OH-Pyrimidine, D_2O exchangeable), δ 9.74 (s, 1H, NH-Pyrazole, D_2O exchangeable), δ 9.68-9.69 (s, 2H, CONH_2 -Ar., D_2O exchangeable), δ 7.31- 8.15 (m, 3H, -CH-Ar.), δ 5.80 (s, 1H, -CH-Pyrimidine), δ 2.50 (s, 3H, - CH_3 -Pyrimidine); ^{13}C NMR (400 MHz, DMSO- d_6 , δ ppm) : 165.55, 164.45, 154.65, 152.83, 149.09, 140.85, 140.44, 131.12, 131.04, 130.52, 130.45, 121.51, 118.04, 117.40, 117.26, 98.49, 86.44, 86.29, 18.82, 16.61; LCMS (M/Z) Calculated for $\text{C}_{14}\text{H}_{11}\text{Cl}_2\text{N}_5\text{O}_2$: 351.1; Obtained MS (M/Z): 352.2 (M+1), 354.3 (M+2)

4.1.5.9. 2-((2,4-Dimethylphenyl)amino)-N-(4-ethoxyphenyl)-7-hydroxy-5-methylpyrazolo[1,5-a]pyrimidine-3-carboxamide (6i)

White solid; Yield 78.12%; M. P. 271-273 °C; IR (KBr, cm^{-1}) 3334 (-NH str.) 1668 (-CO-NH str.), 1238 (C-N str.), 1049 (C-O-C); ^1H NMR (400 MHz, DMSO- d_6 , δ ppm) : δ 11.96 (s, 1H, OH-Pyrimidine, D_2O exchangeable), δ 9.52 (s, 1H, CONH-Ar., D_2O exchangeable), δ 8.96

(s, 1H, NH-Pyrazole, D₂O exchangeable), δ 6.92- 8.23 (m, 7H, -CH-Ar.) , δ 5.78 (s, 1H, -CH-Pyrimidine), δ 2.35-3.58 (s, 5H, -OC₂H₅-Ar.), δ 2.23 (s, 6H, -CH₃-Ar.), δ 1.31-1.34 (s, 3H, -CH₃-Pyrimidine); ¹³C NMR (400 MHz, DMSO-d₆, δ ppm) : 161.78, 154.94, 154.89, 153.69, 149.73, 139.83, 136.61, 131.25, 130.64, 129.02, 126.89, 123.96, 122.87, 116.83, 114.21, 98.25, 87.02, 63.10, 20.27, 18.84, 17.43, 14.64; LCMS (M/Z)Calculated for C₂₄H₂₅N₅O₃: 431.2; Obtained MS (M/Z): 432.4 (M+1)

4.1.5.10. *N*-(4-Chlorophenyl)-2-((2,4-dimethylphenyl)amino)-7-hydroxy-5-methylpyrazolo[1,5-a]pyrimidine-3-carboxamide (6j)

White solid; Yield 65.13%; M. P. 298-300 °C;IR (KBr, cm⁻¹) 3352 (-NH str.), 1662 (-CO-NH str.), 1230 (C-N str.), 819, 578 (C-Cl); ¹H NMR (400 MHz, DMSO-d₆, δ ppm) : δ 12.02 (s, 1H, OH-Pyrimidine, D₂O exchangeable), δ 9.82 (s, 1H, CONH-Ar., D₂O exchangeable), δ 8.79 (s, 1H, NH-Pyrazole, D₂O exchangeable), δ 7.00- 8.22 (m, 7H, -CH-Ar.), δ 5.80 (s, 1H, -CH-Pyrimidine), δ 2.24 (s, 3H, -CH₃-Pyrimidine), δ 2.23 (s, 6H, -CH₃-Ar.); ¹³C NMR (400 MHz, DMSO-d₆, δ ppm) : 162.04, 154.85, 153.59, 149.82, 140.05, 137.59, 136.48, 130.65, 128.17, 128.41, 127.14, 126.89, 124.04, 122.41, 116.93, 98.40, 87.09, 20.28, 18.85, 17.40; LCMS (M/Z)Calculated for C₂₂H₂₀ClN₅O₂: 421.1; Obtained MS (M/Z): 422.2 (M+1) 424.6 (M+2)

4.1.5.11. *N*-(2,4-Dimethylphenyl)-7-hydroxy-2-((4-methoxyphenyl)amino)-5-methylpyrazolo[1,5-a]pyrimidine-3-carboxamide (6k)

White solid; Yield 85.43%; M. P. 288-290°C;IR (KBr, cm⁻¹) 3344 (-NH str.), 1660 (-CO-NH str.), 1244 (C-N str.), 1039 (C-O-C); ¹H NMR (400 MHz, DMSO-d₆, δ ppm) : δ 11.72 (s, 1H, OH-Pyrimidine, D₂O exchangeable), δ 9.09 (s, 1H, CONH-Ar., D₂O exchangeable), δ 9.93 (s, 1H, NH-Pyrazole, D₂O exchangeable), δ 6.88- 7.54 (m, 7H, -CH-Ar.), δ 6.87 (s, 1H, -CH-Pyrimidine), δ 3.64 (s, 3H, -OCH₃-Ar.), δ 2.36 (s, 3H, -CH₃-Pyrimidine), δ 2.19-2.28 (s, 6H, -CH₃-Ar.); ¹³C NMR (400 MHz, DMSO-d₆, δ ppm) : 161.55, 154.79, 153.54, 134.58, 133.53, 130.85, 126.52, 125.03, 118.53, 114.10, 98.40, 87.18, 55.14, 20.49, 18.88, 17.89; LCMS (M/Z)Calculated for C₂₃H₂₃N₅O₃: 417.1; Obtained(M/Z): 418.4 (M+1), 419.2 (M+2)

4.1.5.12. 2-((3,4-Dichlorophenyl)amino)-N-(2,3-dimethylphenyl)-7-hydroxy-5-methylpyrazolo[1,5-a]pyrimidine-3-carboxamide (6l)

Yellow solid; Yield 89.47%; M. P. 282-285°C;IR (KBr, cm⁻¹) 3350 (-NH str.), 1668 (-CO-NH str.), 1278 (C-N str.), 821, 661 (C-Cl); ¹H NMR (400 MHz, DMSO-d₆, δ ppm) : δ 11.82 (s, 1H, OH-Pyrimidine, D₂O exchangeable), δ 9.41 (s, 1H, CONH-Ar., D₂O exchangeable), δ 9.28 (s, 1H, NH-Pyrazole, D₂O exchangeable), δ 7.07- 8.94 (m, 6H, -CH-Ar.), δ 5.83 (s, 1H, -CH-Pyrimidine), δ 2.33 (s, 3H, -CH₃-Pyrimidine), δ 2.29-2.20 (s, 6H, -CH₃-Ar.); ¹³C NMR

(400 MHz, DMSO-d₆, δ ppm) : 161.46, 152.43, 141.12, 136.99, 135.79, 131.04, 130.49, 127.26, 125.27, 121.47, 118.06, 117.39, 87.55, 20.19, 14.35; LCMS (M/Z) Calculated for C₂₂H₁₉Cl₂N₅O₂: 455.0; Obtained MS (M/Z): 456.4 (M+1), 458.5 (M+2)

4.1.5.13. 2-((2,4-Dimethylphenyl)amino)-N-(4-fluorophenyl)-7-hydroxy-5-methylpyrazolo[1,5-a]pyrimidine-3-carboxamide (6m)

Pale yellow solid; Yield 68.16 %; M. P. 275-278 °C; IR (KBr, cm⁻¹) 3361 (-NH str.), 1658 (-CO-NH str.), 1207 (C-N str.), 833, 1159 (C-F); ¹H NMR (400 MHz, DMSO-d₆, δ ppm) : δ 11.99 (s, 1H, OH-Pyrimidine, D₂O exchangeable), δ 9.91 (s, 1H, CONH-Ar., D₂O exchangeable), δ 9.74 (s, 1H, NH-Pyrazole, D₂O exchangeable), δ 5.80- 9.24 (m, 7H, -CH-Ar.), δ 4.10 (s, 1H, -CH-Pyrimidine), δ 2.50 (s, 3H, -CH₃-Ar.), δ 2.36 (s, 3H, -CH₃-Pyrimidine), δ 2.32-2.23 (s, 6H, -CH₃-Ar.); ¹³C NMR (400 MHz, DMSO-d₆, δ ppm) : 162.04, 154.85, 153.59, 149.82, 140.05, 137.59, 136.48, 130.65, 128.17, 128.41, 127.14, 126.89, 124.04, 122.41, 116.93, 98.40, 87.09, 20.28, 18.85, 17.40; LCMS (M/Z) Calculated for C₂₂H₂₀FN₅O₂: 405.4; Obtained MS (M/Z): 406.4 (M+1);

4.1.5.14. 7-Hydroxy-N-(2-methoxyphenyl)-5-methyl-2-(m-tolylamino)pyrazolo[1,5-a]pyrimidine-3-carboxamide (6n)

White solid; Yield 82.45%; M. P. 240-243 °C; IR (KBr, cm⁻¹) 3346 (-NH str.), 1674 (-CO-NH str.), 1247 (C-N str.), 1027 (C-O-C); ¹H NMR (400 MHz, DMSO-d₆, δ ppm) : δ 11.79 (s, 1H, OH-Pyrimidine, D₂O exchangeable), δ 9.31 (s, 1H, CONH-Ar., D₂O exchangeable), δ 8.82 (s, 1H, NH-Pyrazole, D₂O exchangeable), δ 6.70- 8.16 (m, 8H, -CH-Ar.), δ 5.83 (s, 1H, -CH-Pyrimidine), δ 3.84 (s, 3H, -CH₃-Ar.), δ 2.40 (s, 3H, -CH₃-Ar.), δ 2.26 (s, 3H, -CH₃-Pyrimidine); ¹³C NMR (400 MHz, DMSO-d₆, δ ppm) : 161.79, 155.70, 153.71, 138.99, 136.17, 131.38, 125.68, 122.86, 122.67, 122.56, 115.24, 113.72, 55.20, 20.47, 12.91; LCMS (M/Z) Calculated for C₂₂H₂₁N₅O₃: 403.4; Obtained MS (M/Z): 404.3 (M+1)

4.1.5.15. 2-((4-Chlorophenyl)amino)-7-hydroxy-5-methylpyrazolo[1,5-a]pyrimidine-3-carboxamide (6o)

Brown solid; Yield 43.67%; M. P. 320-326 °C; IR (KBr, cm⁻¹) 3475, 3172 (-N-H str.), 1685 (-CO-N-H str.), 1290 (C-N str.), 806, 667 (C-Cl); ¹H NMR (400 MHz, DMSO-d₆, δ ppm) : δ 11.57 (s, 1H, OH-Pyrimidine, D₂O exchangeable), δ 9.65 (s, 1H, NH-Pyrazole, D₂O exchangeable), δ 7.68-7.71 (s, 2H, CONH₂-Ar., D₂O exchangeable), δ 7.33- 7.67 (m, 4H, -CH-Ar.), δ 5.78 (s, 1H, -CH-Pyrimidine), δ 2.34 (s, 3H, -CH₃-Pyrimidine); ¹³C NMR (400 MHz, DMSO-d₆, δ ppm) : 165.55, 164.45, 154.65, 152.83, 149.09, 140.85, 140.44, 131.12, 131.04, 130.52, 130.45, 121.51, 118.04, 117.40, 117.26, 98.49, 86.44, 86.29, 18.82, 16.61;

LCMS (M/Z) Calculated for C₁₄H₁₂ClN₅O₂: 317.7; Obtained MS (M/Z): 318.4 (M+1) 320.3 (M+2)

4.1.5.16. 2-((3,4-Difluorophenyl)amino)-N-(4-fluorophenyl)-7-hydroxy-5-methylpyrazolo[1,5-a]pyrimidine-3-carboxamide (6p)

Yellow solid; Yield 68.19%; M. P. 290-294°C; IR (KBr, cm⁻¹) 3363 (-NH str.), 1652 (-CO-NH str.), 1271 (C-N str.), 833, 1159 (C-F); ¹H NMR (400 MHz, DMSO-d₆, δ ppm) : δ 11.98 (s, 1H, OH-Pyrimidine, D₂O exchangeable), δ 9.91 (s, 1H, CONH-Ar., D₂O exchangeable), δ 8.88 (s, 1H, NH-Pyrazole, D₂O exchangeable), δ 6.48- 8.02 (m, 7H, -CH-Ar.), δ 5.79 (s, 1H, -CH-Pyrimidine), δ 2.35 (s, 3H, -CH₃-Pyrimidine); ¹³C NMR (400 MHz, DMSO-d₆, δ ppm) : 160.99, 159.44, 157.05, 154.75, 152.24, 150.37, 147.97, 144.61, 142.36, 142.24, 140.45, 138.24, 138.14, 135.10, 122.56, 122.49, 117.35, 117.17, 115.17, 114.95, 113.38, 106.07, 105.85, 98.16, 87.90, 18.85, 16.66; LCMS (M/Z) Calculated for C₂₀H₁₄F₃N₅O₂: 413.3; Obtained MS (M/Z): 414.4 (M+1)

4.1.5.17. N-(4-Ethoxyphenyl)-7-hydroxy-5-methyl-2-(phenylamino)pyrazolo[1,5-a]pyrimidine-3-carboxamide (6q)

White solid; Yield 72.55%; M. P. 280-284°C; IR (KBr, cm⁻¹) 3377 (-NH str.), 1652 (-CO-NH str.), 1294 (C-N str.), 1047 (C-O-C); ¹H NMR (400 MHz, DMSO-d₆, δ ppm) : δ 11.92 (s, 1H, OH-Pyrimidine, D₂O exchangeable), δ 9.58 (s, 1H, CONH-Ar., D₂O exchangeable), δ 8.89 (s, 1H, NH-Pyrazole, D₂O exchangeable), δ 6.89- 7.67 (m, 9H, -CH-Ar.), δ 5.77 (s, 1H, -CH-Pyrimidine), δ 2.35-3.46 (s, 5H, -OC₂H₅-Ar.), δ 1.32 (s, 3H, -CH₃-Pyrimidine); ¹³C NMR (400 MHz, DMSO-d₆, δ ppm) : 161.15, 154.84, 152.84, 140.94, 131.47, 128.80, 122.54, 120.40, 117.03, 114.17, 98.14, 87.71, 63.09, 18.84, 14.65; LCMS (M/Z) Calculated for C₂₂H₂₁N₅O₃: 403.4; Obtained MS (M/Z): 404.3 (M+1)

4.1.5.18. N-(2,3-Dichlorophenyl)-2-(4-ethylpiperazin-1-yl)-7-hydroxy-5-methylpyrazolo[1,5-a]pyrimidine-3-carboxamide (6r)

White solid; Yield 39.20%; M. P. 268-269°C; IR (KBr, cm⁻¹) 3323 (-NH str.), 1663 (-CO-NH str.), 1240 (C-N str.), 1033 (-C-O-C), 829 (P-substituted), 775 (-C-Cl str.); ¹H NMR (400 MHz, DMSO-d₆, δ ppm) : δ 11.96 (s, 1H, OH-Pyrimidine, D₂O exchangeable), δ 9.41 (s, 1H, CONH-Ar., D₂O exchangeable), δ 7.07- 8.09 (m, 3H, -CH-Ar.), δ 5.83 (s, 1H, -CH-Pyrimidine), δ 2.57-3.34 (s, 5H, -OC₂H₅-Ar.), δ 1.88 (s, 3H, -CH₃-Pyrimidine), δ 1.34 (s, 2H, -CH₂-N-ethyl piperazine), δ 1.34 (s, 4H, -CH₃-N-ethyl piperazine), δ 1.32 (s, 3H, -CH₃-Ar.); ¹³C NMR (400 MHz, DMSO-d₆, δ ppm) : 159.88, 154.84, 152.94, 131.47, 128.80, 20.80, 113.83, 90.21, 65.85, 55.17, 16.51; LCMS (M/Z) Calculated for C₂₀H₂₂ClN₅O₂: 449.3; Obtained MS (M/Z): 449.4 (M), 451.4 (M+2), 453.1 (M+4)

4.1.5.19. *N*-(3,4-Dichlorophenyl)-7-hydroxy-5-methyl-2-(pyrrolidin-1-yl)pyrazolo[1,5-*a*]pyrimidine-3-carboxamide (6s)

White solid; Yield 68.22%; M. P. 273-275°C; IR (KBr, cm^{-1}) 3350 (-NH str.), 1662 (-CO-NH str.), 1298 (-C-N str.), 892 (Di-substituted), 840 (*P*-substituted), 750 (-C-Cl str.); ^1H NMR (400 MHz, DMSO- d_6 , δ ppm) : δ 11.82 (s, 1H, OH-Pyrimidine, D_2O exchangeable), δ 9.41 (s, 1H, CONH-Ar., D_2O exchangeable), δ 7.07- 7.57 (m, 3H,-CH-Ar.), δ 5.83 (s, 1H,-CH-Pyrimidine), δ 3.50-1.88 (s, 5H, -OC $_2$ H $_5$ -Ar.), δ 1.88 (s, 4H, CH $_2$ pyrrolidine ring), δ 1.34 (s, 4H, CH $_2$ pyrrolidine ring), δ 1.34 (s, 3H, -CH $_3$ -Pyrimidine); ^{13}C NMR (400 MHz, DMSO- d_6 , δ ppm) : 159.88, 155.57, 154.82, 153.49, 153.21, 147.20, 140.30, 120.80, 113.83, 90.21, 65.85, 55.17, 16.51; LCMS (M/Z) Calculated for C $_{18}$ H $_{17}$ Cl $_2$ N $_5$ O $_2$: 406.2; Obtained MS (M/Z): 406.4 (M), 408.2 (M+2), 410.1 (M+4)

4.1.5.20. 7-Hydroxy-5-methyl-*N*-phenyl-2-(phenylamino)pyrazolo[1,5-*a*]pyrimidine-3-carboxamide (6t)

White solid; Yield 84.24%; M. P. 280-284°C; IR (KBr, cm^{-1}) 3348 (-NH str.), 1662 (-CO-NH str.), 1298 (-C-N str.), 840 (*P*-substituted); ^1H NMR (400 MHz, DMSO- d_6 , δ ppm) : δ 11.99 (s, 1H, OH-Pyrimidine, D_2O exchangeable), δ 9.77 (s, 1H, CONH-Ar., D_2O exchangeable), δ 8.80 (s, 1H, NH-Pyrazole, D_2O exchangeable), δ 6.89- 7.69 (m, 10H,-CH-Ar.), δ 5.78 (s, 1H,-CH-Pyrimidine), δ 3.37 (s, 3H, -CH $_3$ -Pyrimidine); ^{13}C NMR (400 MHz, DMSO- d_6 , δ ppm) : 161.47, 154.83, 152.99, 149.87, 140.42, 138.69, 138.48, 129.18, 128.46, 123.52, 120.81, 117.15, 98.21, 87.69, 20.30; LCMS (M/Z) Calculated for C $_{20}$ H $_{17}$ N $_5$ O $_2$: 359.3; Obtained MS (M/Z): 360.3 (M+1)

4.1.5.21. 7-Hydroxy-5-methyl-*N*-phenyl-2-(*p*-tolylamino)pyrazolo[1,5-*a*]pyrimidine-3-carboxamide (6u)

White solid; Yield 49.12%; M. P. 274-276°C; IR (KBr, cm^{-1}) 3365 (-NH str.), 1660 (-CO-NH str.), 1228 (-C-N str.), 817 (*P*-substituted); ^1H NMR (400 MHz, DMSO- d_6 , δ ppm) : δ 11.99 (s, 1H, OH-Pyrimidine, D_2O exchangeable), δ 9.77 (s, 1H, CONH-Ar., D_2O exchangeable), δ 8.80 (s, 1H, NH-Pyrazole, D_2O exchangeable), δ 6.89- 7.69 (m, 10H,-CH-Ar.), δ 5.78 (s, 1H,-CH-Pyrimidine), δ 2.35 (s, 3H, -CH $_3$ -Ar), δ 2.08 (s, 3H, -CH $_3$ -Pyrimidine); ^{13}C NMR (400 MHz, DMSO- d_6 , δ ppm) : 161.47, 154.83, 152.99, 149.87, 140.42, 138.69, 138.48, 129.18, 128.46, 123.52, 120.81, 117.15, 98.21, 87.69, 20.30, 18.83; LCMS (M/Z) Calculated for C $_{21}$ H $_{19}$ N $_5$ O $_2$: 373.4; Obtained MS (M/Z): 374.3 (M+1)

4.1.5.22. 2-((4-Chlorophenyl)amino)-7-hydroxy-5-methyl-*N*-phenylpyrazolo[1,5-*a*]pyrimidine-3-carboxamide (6v)

Pale yellow solid; Yield 51.12%; M. P. 266-268°C; IR (KBr, cm^{-1}) 3365 (-NH str.), 1660 (-CO-NH str.), 1294 (-C-N str.), 821 (*P*-substituted), 754 (-C-Cl str.); ^1H NMR (400 MHz, DMSO- d_6 , δ ppm) : δ 11.99 (s, 1H, OH-Pyrimidine, D_2O exchangeable), δ 9.77 (s, 1H, CONH-Ar., D_2O exchangeable), δ 8.80 (s, 1H, NH-Pyrazole, D_2O exchangeable), δ 6.89-7.69 (m, 10H, -CH-Ar.), δ 5.78 (s, 1H, -CH-Pyrimidine), δ 2.50 (s, 3H, -CH₃-Pyrimidine); ^{13}C NMR (400 MHz, DMSO- d_6 , δ ppm) : 161.22, 154.81, 152.42, 150.09, 140.48, 139.94, 138.71, 128.90, 128.72, 128.51, 128.47, 123.81, 123.54, 120.75, 118.97, 118.66, 98.16, 88.05, 18.85, 16.71; LCMS (M/Z) Calculated for $\text{C}_{20}\text{H}_{16}\text{ClN}_5\text{O}_2$: 393.8; Obtained MS (M/Z): 394.3 (M+1), 396.3 (M+2)

4.1.5.23. *N*-(3-Chloro-4-fluorophenyl)-7-hydroxy-5-methyl-2-(*p*-tolylamino)pyrazolo[1,5-*a*]pyrimidine-3-carboxamide (6w)

White solid; Yield 59.29%; M. P. 265-269°C; IR (KBr, cm^{-1}) 3346 (-NH str.), 1649 (-CO-NH str.), 1207 (-C-N str.), 1130 (-C-F str.), 867 (D-substituted), 821 (*P*-substituted), 766 (-C-Cl str.); ^1H NMR (400 MHz, DMSO- d_6 , δ ppm) : δ 11.90 (s, 1H, OH-Pyrimidine, D_2O exchangeable), δ 9.92 (s, 1H, CONH-Ar., D_2O exchangeable), δ 8.53 (s, 1H, NH-Pyrazole, D_2O exchangeable), δ 6.87- 7.96 (m, 7H, -CH-Ar.), δ 5.76 (s, 1H, -CH-Pyrimidine), δ 3.72 (s, 3H, -CH₃-Ar), δ 2.34 (s, 3H, -CH₃-Pyrimidine); ^{13}C NMR (400 MHz, DMSO- d_6 , δ ppm) : 161.50, 154.89, 154.43, 152.96, 152.01, 149.93, 140.63, 138.35, 136.03, 136.00, 129.24, 129.08, 122.00, 120.91, 118.95, 118.77, 117.28, 116.69, 98.29, 87.34, 20.28, 18.94, 13.94; LCMS (M/Z) Calculated for $\text{C}_{21}\text{H}_{17}\text{ClFN}_5\text{O}_2$: 425.8; Obtained MS (M/Z): 426.3 (M+1)

4.1.5.24. *N*-(3-Chloro-4-fluorophenyl)-7-hydroxy-2-((4-methoxyphenyl)amino)-5-methylpyrazolo[1,5-*a*]pyrimidine-3-carboxamide (6x)

Yellow solid; Yield 68.41%; M. P. 260-263°C; IR (KBr, cm^{-1}) 3390 (-NH str.), 1641 (-CO-NH str.), 1259 (-C-N str.), 1163 (-C-F str.), 1036 (-C-O-C), 877 (D-substituted), 819 (*P*-substituted), 738 (-C-Cl str.); ^1H NMR (400 MHz, DMSO- d_6 , δ ppm) : δ 11.90 (s, 1H, OH-Pyrimidine, D_2O exchangeable), δ 9.92 (s, 1H, CONH-Ar., D_2O exchangeable), δ 8.53 (s, 1H, NH-Pyrazole, D_2O exchangeable), δ 6.87- 7.96 (m, 7H, -CH-Ar.), δ 5.76 (s, 1H, -CH-Pyrimidine), δ 3.58 (s, 3H, -OCH₃-Ar), δ 2.34 (s, 3H, -CH₃-Pyrimidine); ^{13}C NMR (400 MHz, DMSO- d_6 , δ ppm) : 161.50, 154.89, 154.43, 152.96, 152.01, 149.93, 140.63, 138.35, 136.03, 136.00, 129.24, 129.08, 122.00, 120.91, 118.95, 118.77, 117.28, 116.69, 98.29, 87.34, 55.20, 20.28, 18.94; LCMS (M/Z) Calculated for $\text{C}_{21}\text{H}_{17}\text{ClFN}_5\text{O}_3$: 441.8; Obtained MS (M/Z): 442.3 (M+1), 443.2 (M+2), 444.4 (M+3)

4.1.5.25. *N*-(3-Chlorophenyl)-2-((4-fluorophenyl)amino)-7-hydroxy-5-methylpyrazolo[1,5-*a*]pyrimidine-3-carboxamide (6y)

Yellow solid; Yield 74.44%; M. P. 254-256°C; IR (KBr, cm^{-1}) 3388 (-NH str.), 1643 (-CO-NH str.), 1215 (-C-N str.), 1161 (-C-F str.), 827 (*P*-substituted), 775 (-C-Cl str.); ^1H NMR (400 MHz, DMSO- d_6 , δ ppm) : δ 11.96 (s, 1H, OH-Pyrimidine, D_2O exchangeable), δ 9.95 (s, 1H, CONH-Ar., D_2O exchangeable), δ 8.72 (s, 1H, NH-Pyrazole, D_2O exchangeable), δ 7.11- 7.86 (m, 8H, -CH-Ar.), δ 5.78 (s, 1H, -CH-Pyrimidine), δ 2.35 (s, 3H, -CH₃-Pyrimidine); ^{13}C NMR (400 MHz, DMSO- d_6 , δ ppm) : 161.38, 157.71, 155.36, 154.74, 152.61, 150.01, 140.67, 140.37, 137.43, 132.76, 130.15, 123.02, 119.93, 118.86, 118.75, 118.68, 115.27, 115.05, 98.27, 87.73, 18.8; LCMS (M/Z) Calculated for $\text{C}_{20}\text{H}_{15}\text{ClFN}_5\text{O}_2$: 411.8; Obtained MS (M/Z): 412.3 (M+1), 414.4 (M+2);

4.1.5.26. *N*-(3-Chlorophenyl)-2-((2,3-dimethylphenyl)amino)-7-hydroxy-5-methylpyrazolo[1,5-*a*]pyrimidine-3-carboxamide (6z)

White solid; Yield 76.86 %; M. P. 264-266 °C; IR (KBr, cm^{-1}) 3348 (-NH str.), 1656 (-CO-NH str.), 1234 (-C-N str.), 827 (*P*-substituted), 773 (-C-Cl str.); ^1H NMR (400 MHz, DMSO- d_6 , δ ppm) : δ 12.03 (s, 1H, OH-Pyrimidine, D_2O exchangeable), δ 9.88 (s, 1H, CONH-Ar., D_2O exchangeable), δ 8.85 (s, 1H, NH-Pyrazole, D_2O exchangeable), δ 7.76- 8.16 (m, 7H, -CH-Ar.), δ 5.77 (s, 1H, -CH-Pyrimidine), δ 2.35 (s, 3H, -CH₃-Ar), δ 2.26 (s, 3H, -CH₃-Ar), δ 2.18 (s, 3H, -CH₃-Pyrimidine); ^{13}C NMR (400 MHz, DMSO- d_6 , δ ppm) : 162.20, 154.96, 153.71, 140.18, 138.86, 136.17, 132.80, 130.22, 125.61, 123.06, 122.91, 122.70, 120.08, 119.05, 115.47, 98.33, 87.14, 20.45, 18.92, 12.92; LCMS (M/Z) Calculated for $\text{C}_{22}\text{H}_{20}\text{ClN}_5\text{O}_2$: 421.8; Obtained MS (M/Z): 422.4 (M+1), 424.4 (M+2)

4.2. Molecular docking study

4.2.1. Ligand Preparation, Protein preparation and grid generation

Molecular docking, a part of computer aided-drug design approach which having crucial role in the construction of potential lead molecules via interactions with key amino acid residues of identified targeted protein structure. Newly designed NCE's surviving to the Lipinski's rule of five (**6a-6z**) were minimized and docked using "Glide Extra precision" (XP) protocol to identify vital amino acid residues (Maestro v10.1, Schrodinger, LLC, NEW YORK, NY). For the preparation of protein structure of enoyl-ACP reductases (InhA) inhibitor with co-crystalline structure (PDB IDs: 2H7M) was selected and extracted from protein data bank (PDB <http://www.rcsb.org/pdb>). Further for the refinement of the protein "Protein Preparation Wizard" in Maestro (Maestro v.10.1) was applied followed by addition of the hydrogen atoms and removal of the water molecules beyond 5 Å with OPLS 2005 force field. Further "Glide's Receptor Grid Generation" module was used to generate the receptor grid at

the active site of co-crystalline ligand with the centred dimension cubic box of $10 \text{ \AA} \times 10 \text{ \AA} \times 10 \text{ \AA}$ [24].

4.3. *In-silico* ADME prediction

Acceptable ADMET profile is one of the imperative measures for the accomplishment of drug. Pyrazole derivatives obtained through molecular docking study further opted for *in-silico* ADMET prediction using QikProp module in Schrodinger to check its druggability[20]. This module predicts physical descriptors like molecular weight, partition coefficient, cell permeability, partition coefficient to brain/blood, blockage of HERG K⁺ channels, number of metabolic reactions and percentage human oral absorption and mutagenicity compared to the properties of a particular known standard drugs. Small molecules that comply with Lipinski's rule of five were further opted for the synthesis.

4.4. *Biological Evaluation*

4.4.1. *In-vitro* anti-tubercular activity

Micro plate Alamar Blue Assay (MABA) is a non-toxic method which is most commonly uses thermally stable reagents. It includes Resazurin, oxidized form of Alamar blue on inoculation of tubercle bacilli reduces to resorufin and gives fluorescent pink colour. The newly synthesized final analogues of 7-hydroxy-5-methyl-N-substitutedphenyl-2-(substituted phenylamino)pyrazolo[1,5-*a*]pyrimidine-3-carboxamide(**6a-6z**) were screened for its *in-vivo* anti-mycobacterial activity against H37Rv strain using Micro plate Alamar Blue Assay method [25]. Ciprofloxacin, Pyrazinamide and Streptomycin were used as reference standard drugs. To minimize evaporation of medium in the test wells during incubation 200µl sterile deionized water was added in 96 wells plate. To that 100 µl of the Middle brook 7H9 broth and serial dilutions of compounds with 100 to 0.2 µg/ml concentration were added to the plate. These plates were covered with Para film and incubated at 37°C for five days. To this 25µl of freshly prepared 1:1 mixture of Alamar Blue reagent and 10% tween 80 was added to the plate and incubated for 24 hrs. A blue colour in the well was interpreted as no bacterial growth, and pink colour was recorded as growth and the MIC was defined as lowest drug concentration which prevented the colour change from blue to pink.

4.4.2. *MDR-TB and XDR-TB* study

Additionally MDR-TB and XDR-TB study was performed using Lowenstein-Jensen medium (L. J. medium) on H37Rv strain with potent heat molecules based on *in-vitro* Micro plate Alamar Blue Assay method [26]. This method used to check the susceptibility of the compounds with the strain of multidrug-resistant TB and extensively drug-resistant TB. 4 mL of sterilized malachite green solution was added to the solution of aseptically broken eggs. To

that mineral salt solution was added which consist of magnesium sulphate (0.4 g), magnesium citrate (1.6 g), potassium phosphate (4.0 g), asparagine (6.0 g), glycerol (20 mL) and make up the volume up to 1000 mL with distilled water and mixed well to form uniform medium. Further synthesized targeted compounds dissolved in 10 mL DMSO and from that 0.8 mL of each concentration was transferred into different McCartney bottles. To this 7.2 mL of L. J. medium was added and mixed well and bottles were incubated at 75°C - 80°C for 3 days for solidification. Isoniazid was considered as a reference standard for the comparison of anti-tubercular activity.

4.4.3. MTT Cytotoxicity activity

Compounds active to anti-tubercular study (with MIC < 12.5µg/mL) were further evaluated against mammalian Vero cell line for cytotoxicity study [27]. Vero Cell line was obtained from National Centre for Cell Sciences (NCCS), Pune. Cell viability was assessed after exposure to 72 h on the basis of cellular conversion of formazan product from MTT using the Promega Cell Titer 96 non-radioactive cell proliferation assay. The obtained results are important for the development of new chemical entities for the treatment of TB.

4.5. Molecular Dynamics simulation

The molecular dynamics study was performed with Berendsen thermostat and barostat methods for 10 ns for the best dock protein-ligand complex using DESMOND (Schrodinger Inc., USA) module [28]. The molecular dynamics simulation system study desired protein-ligand complex was saturated and partial charges were determined. Energy minimization was performed using OPLS_2005 force field [29]. The solvated system inserted to TIP3P orthorhombic box of 10 Å × 10 Å × 10 Å [30]. Each system was then neutralised by the system-built option in the protocol by adding 0.15 M NaCl in buffer. The precision of the chemical structures was confirmed by Protein Preparation, Ligand preparation, and Epik tools provided in Desmond. The minimized explicit solvation complex of ligand receptor complex was simulated for 10 ns using NPT ensemble (temperature of 300 K and pressure of 1.01325 bars) [31]. Steepest Descent and Broyden-Fletcher-Goldfarb-Shanno algorithms were applied to achieve the relaxation of the system. Dynamics simulation process was maintained 300 K temperature and 1 atm pressure with Nose-Hoover thermostat algorithm and Martyna Tobias-Klein algorithm respectively. Long-range and short-range coulombic interaction was controlled using smooth particle mesh ewald method with 9.0 Å endpoint values. MD simulations were performed for 10 ns, and trajectory information was obtained with the rest of 2.0 ns [32]. Plots of RMSD, RMSF and hydrogen bonds were generated along with its dynamic simulation.

Acknowledgments

Authors are thankful to Maratha Mandal's Dental College, Belgaum and NCL Pune for providing biological screening of these titles compounds. Authors are also thankful to Schrodinger Inc. for providing the help for the molecular dynamic simulation study.

Conflict of Interest

The authors declare no conflict of interest about this article.

Supporting Information

All IR-Spectroscopy, MS, ^1H NMR and ^{13}C MR spectra for final derivatives has been provided in the "supplementary content" section.

References

1. M. B. Bhalerao, S. T. Dhumal, A. R. Deshmukh, L. U. Nawale, V. Khedkar, D. Sarkar, R. A. Mane, New Bithiazolylylhydrazones: Novel Synthesis, Characterization and Antitubercular Evaluation, *Bioorg Med Chem Lett* 27 (2017) 288–294.
2. E. Palacios, M. Franke, M. Munoz, R. Hurtado, R. Dallman, K. Chalco, HIV-positive patients treated for multidrug-resistant tuberculosis: Clinical outcomes in HAART era, *Int J Tuberc Lung Dis*.16 (2012) 348-354.
3. A. Bhatt, V. Molle, G. S. Besra, W. R. Jacobs, L. Kremer, The Mycobacterium tuberculosis FAS-II condensing enzymes: their role in mycolic acid biosynthesis, acid-fastness, pathogenesis and in future drug development, *Mol Microbiol*. 6 (2007) 442–1454.
4. S. Smith, A. Witkowski, A. K. Joshi Structural and functional organization of the animal fatty acid synthase, *Prog Lipid Res* 42 (2003) 289–317.
5. R. S. Keri, K. Chand, T. Ramakrishnappa, B. M. Nagaraja, Recent progress on pyrazole scaffold-based antimycobacterial agents, *Arch Pharm* 348 (2015) 299-314.
6. L. Ballell, R. A. Field, K. Duncan, R. J. Young, New small molecule synthetic antimycobacterials, *Antimicrob Agents Chemother* 49 (2005) 2153–2163
7. Y. Janin, Antituberculosis drugs: ten years of research, *Bioorg Med Chem* 15 (2007) 2479–2513

8. T. Jian, W. Bangxing, W. Tian, W. Junting, T. Zhengchao, N. Moses, W. Baojie, G. Scott, T. Franzbluc, Z. Tianyu, D. Ke, Design, Synthesis, and Biological Evaluation of Pyrazolo[1,5-a]pyridine-3-carboxamides as Novel Antitubercular Agents, *ACS Med ChemLett* 6 (2015) 814-818.
9. A. D. Villela, Z. A. Sanchez-Quitian, R. G. Ducati, D. S. Santos, L. A. Basso, Pyrimidine Salvage Pathway in *Mycobacterium tuberculosis*, *Curr Med Chem* 18 (2011) 1286-1298.
10. T. Novinson, B. Bhooshan, T. Okabe, G. R. Revankar, R. K. Robins, K. Senga, H. R. Wilson, Novel heterocyclic nitrofurfuralhydrazones. In vivo antitrypanosomal activity, *J Med Chem* 19 (1976) 512-516.
11. B. Cacciari, B. Chiara, G. Spalluto, K. N. Klotz, M. Bacilieri, F. Deflorian, S. Moro, Pyrazolo-triazolo-pyrimidines as adenosine receptor antagonists: A complete structure-activity profile, *Purinergic Signal* 3 (2007) 183-193
12. S. Selleri, F. Bruni, C. Costagli, A. Costanzo, G. Guerrini, G. Ciciani, P. Gratteri, F. Besnard, B. Costa, M. Montali, A novel selective GABAA $\alpha 1$ receptor agonist displaying sedative and anxiolytic-like properties in rodents, *J Med Chem* 48 (2005) 6756-6760.
13. M. Suzuki, H. Iwasaki, Y. Fujikawa, M. Sakashita, M. Kitahara, R. Sakoda, Synthesis and biological evaluations of condensed pyridine and condensed pyrimidine-based HMG-CoA reductase inhibitors, *Bioorg Med ChemLett* 11 (2001) 1285-1288.
14. M. Fraley, R. S. Rubino, W. F. Hoffman, S. R. Hambaugh, K. L. Arrington, R. W. Hungate, M. T. Bilodeau, A. J. Tebben, R. Z. Rutledge, R. L. Kendall, Optimization of a pyrazolo[1,5-a]pyrimidine class of KDR kinase inhibitors: improvements in physical properties enhance cellular activity and pharmacokinetics, *Bioorg Med ChemLett* 12 (2002) 3537-41.
15. C. Almansa, A. F. De Arriba, F. L. Cavalcanti, L. A. Gómez, A. Miralles, M. Merlos, J. Garcia- Rafanell, J. Forn, Synthesis and SAR of a new series of COX-2-selective inhibitors: Pyrazolo[1,5-a]pyrimidines, *J Med Chem* 44 (2001) 350-361.
16. E. J. Hanan, A. V. Abbema, K. Barrett, W. S. Blair, J. Blaney, C. Chang, C. Eigenbrot, S. Flynn, P. Gibbons, C. A. Hurley, Discovery of potent and selective pyrazolopyrimidine Janus Kinase 2 inhibitors, *J Med Chem* 55 (2012) 10090-10107.
17. Y. Tian, D. Du, D. Rai, L. Wang, H. Liu, P. Zhan, E. D. Clercq, C. Pannecouque, X. Liu, Fused heterocyclic compounds bearing bridge head nitrogen as potent HIV-1NNRTIs. Part 1: Design, synthesis and biological evaluation of novel 5,7-

- disubstituted pyrazolo[1,5-a]pyrimidine derivatives, *Bioorg Med Chem* 22 (2014) 2052–2059.
18. C. Y. Ishak, N. H. Metwally, H. I. Wahbi, In-vitro antimicrobial and antifungal activity of pyrimidine and pyrazolo[1,5-a]pyrimidine, *Int J Pharm Phytopharm Res* 2 (2013) 407–411.
19. L. Xiaoyun, T. Jian, C. Shengyang, W. Baojie, G. Scott, T. Franzblauc, Z. Tianyu, Z. Xiantao, D. Ke, Pyrazolo[1,5-a]pyridine-3-carboxamide hybrids: Design, synthesis and evaluation of anti-tubercular activity, *Eur J Med Chem* 125 (2017) 41-48.
20. M. Palmi, P. Shivani, C. Mahesh, Identification of some novel pyrazolo[1,5-a]pyrimidine derivatives as InhA inhibitors through pharmacophore-based virtual screening and molecular docking, *J BiomolStructDyn* (2018) DOI:10.1080/07391102.2018.1465852.
21. G. H. Elgemeie, A. H. Elghandour, G. W. AbdElaziz, Novel Cyanoketene N,S-Acetals and Pyrazole Derivatives using Potassium 2-Cyanoethylene-1-thiolates, *Synthetic Communications* 37 (2007) 2828-2834.
22. A. Mathews, E. R. Anabha, C. G. Sholly, A Facile Method for the Synthesis of Oxoketene-N,S- and -N,N-acetals from Reactions of Amino Compounds, *Organic Chemistry International Article ID 396020* (2010) 5 pages.
23. T. Kurz, K. Widyan, G. H. Elgemeie, Novel Synthesis of Fluorinated Cyanoketene N,S-Acetals and Their Conversions to Fluorinated Pyrazole Derivatives, *Phosphorus, Sulfur, and Silicon and the Related Elements* 181 (2006) 299-304.
24. X. He, A. Alian, D. M. Ortiz Inhibition of the Mycobacterium enoyl acyl carrier protein reductase InhA by arylamides, *Bioorg & Med Chem* 15 (2007) 6649–6658
25. S. Cho, H. S. Lee, S. Franzblau, Microplate Alamar Blue Assay (MABA) and Low Oxygen Recovery Assay (LORA) for Mycobacterium tuberculosis Methods, *Mol. Biol.* 1285 (2015) 281-92
26. H. Elbir, A. M. Abdel-Muhsin, A. Babiker, A one-step DNA PCR-based method for the detection of Mycobacterium tuberculosis complex grown on Löwenstein–Jensen media, *Am J Trop Med Hyg* 78(2) (2008) 316–317.
27. A. Maria, V. Jhesua, C. Christian, M. Raktim, D. Chandreyee, P. Gloria, J. Homero, N. Valakunja, D. Juan, Diarylethenes displays In vitro Anti-TB Activity and are efficient Hits targeting the Mycobacterium tuberculosis HU Protein, *Molecules* 22 (2017) 1245.

28. A. John, V. Umashankar, S. Krishnakumar, P. R. Deepa, Comparative Modeling and Molecular Dynamics Simulation of Substrate Binding in Human Fatty Acid Synthase: EnoylReductase and β -KetoacylReductase Catalytic Domains, *Genomics Inform* 13 (2015) 15-24.
29. A. W. Schuttelkopf AW, V. Aalten, V PRODRG: a tool for high throughput crystallography of protein-ligand complexes, *ActaCryst D* 60 (2004) 1355–1363.
30. P. Shivani, M. Palmi, R. Vishal, C. Mahesh, Structure-based design, synthesis and evaluation of 2,4-diaminopyrimidine derivatives as novel caspase-1 inhibitors, *BioorgChem* 78 (2018) 258–268.
31. P. Shivani, M. Palmi, C. Mahesh, Rational approach to identify newer caspase-1 inhibitors using pharmacophore based virtual screening, docking and molecular dynamic simulation studies, *JMol GraphModel* 81 (2018) 106-115.
32. G. J. Martyna, Constant-temperature molecular dynamics with momentum conservation, *Phys Rev E Stat.* 50 (1994) 3234-3236.

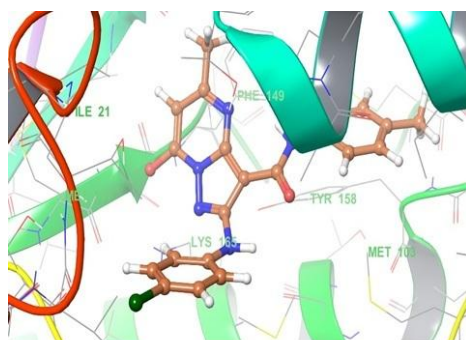


Figure 1(a)

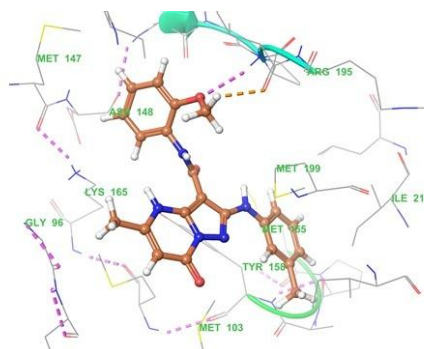


Figure 1(b)

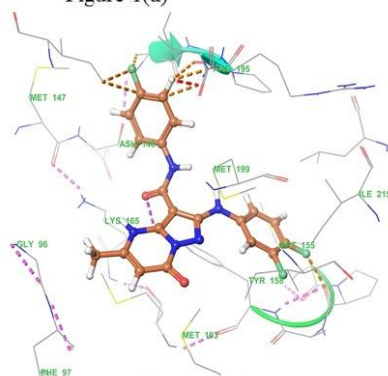


Figure 1(c)

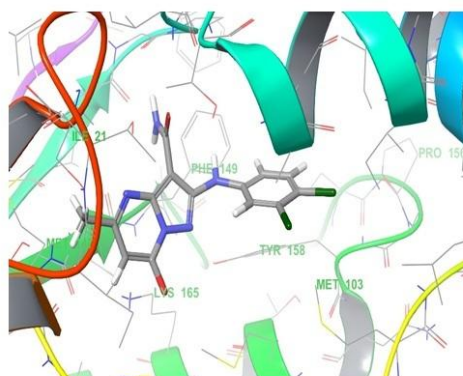


Figure 1(d)

Figure 1. Docking conformation of the most potent inhibitors **6g** (a), **6n** (b), **6p** (c), **6h** (d) with binding pocket of InhA enzyme (PDB : 2H7M)

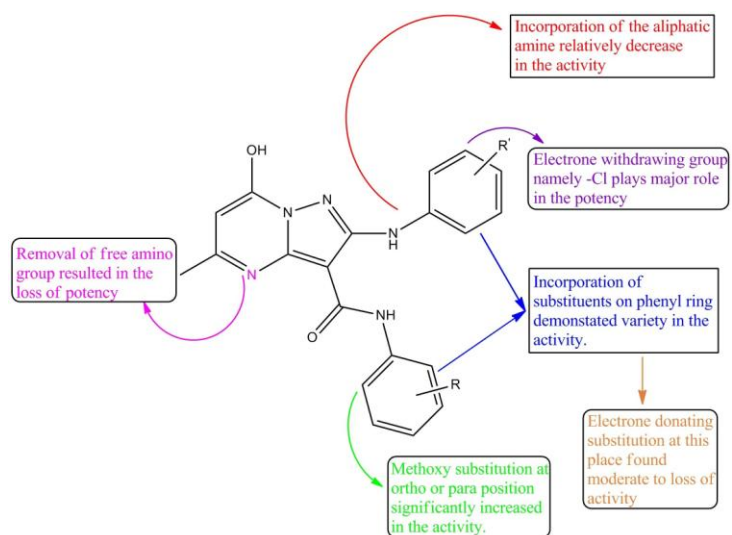


Figure 2. Structure Activity Relationship for pyrazolo[1,5-a]pyrimidine (6a-6z)

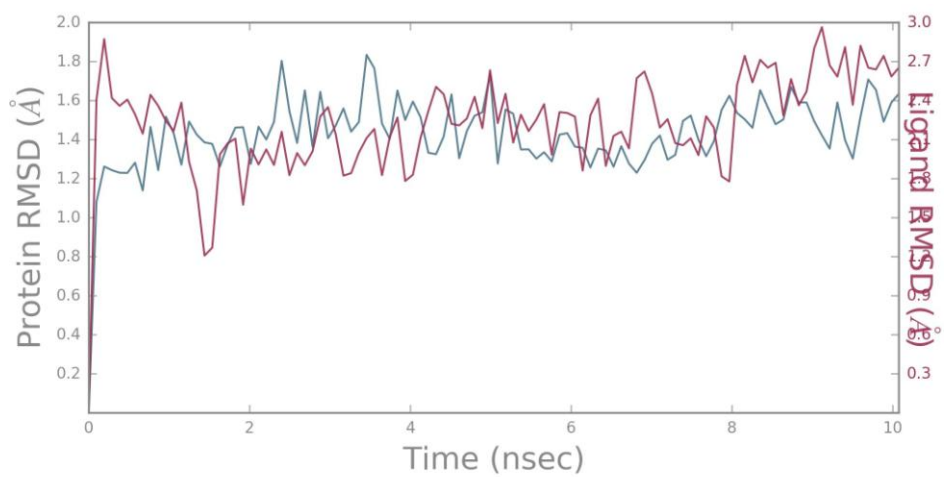


Figure.3(a). Protein-ligand RMSD

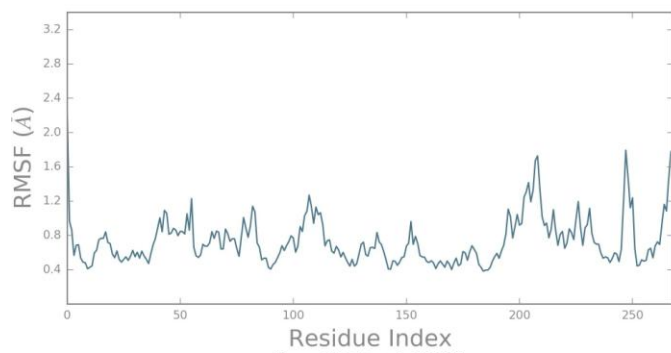


Figure.3(b) Protein RMSF

ACCEPTED MANUSCRIPT

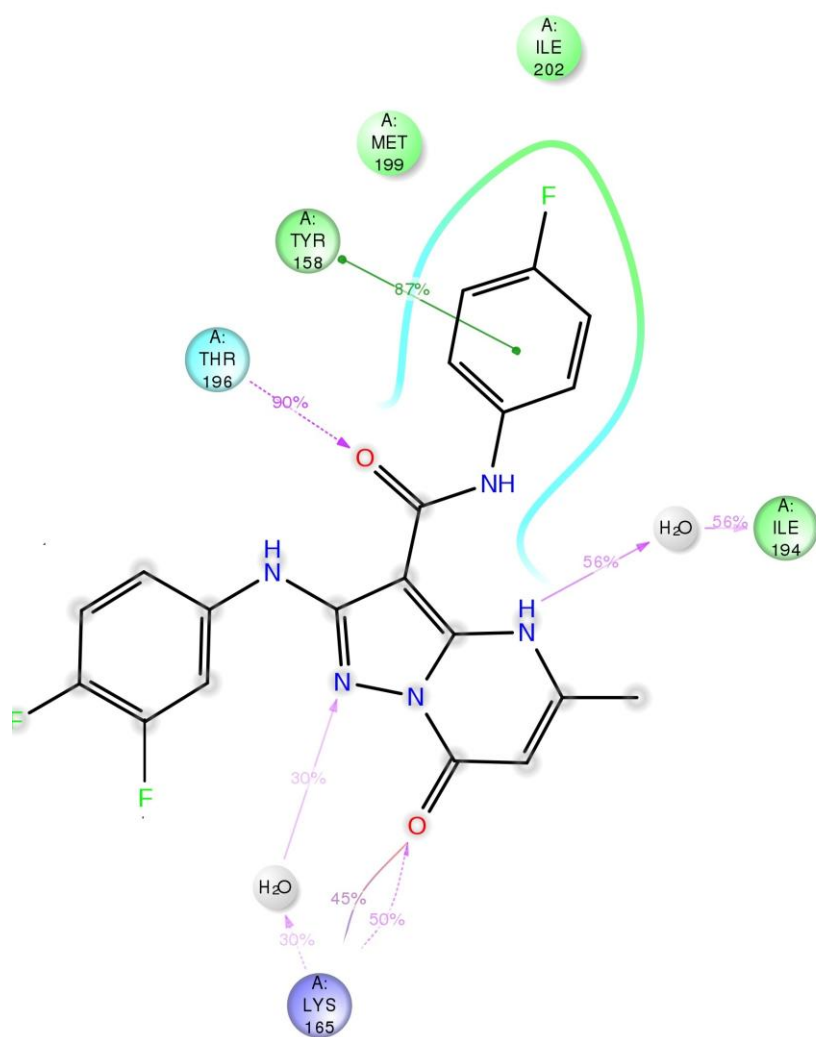


Figure.4. Ligand-protein contact for synthesized compound **6p**

Scheme 1 synthetic approach for the derivatives of 7-hydroxy-5-methyl-N- substituted phenyl-2-(substituted phenylamino)pyrazolo[1,5-*a*]pyrimidine-3-carboxamide (6a-6z)

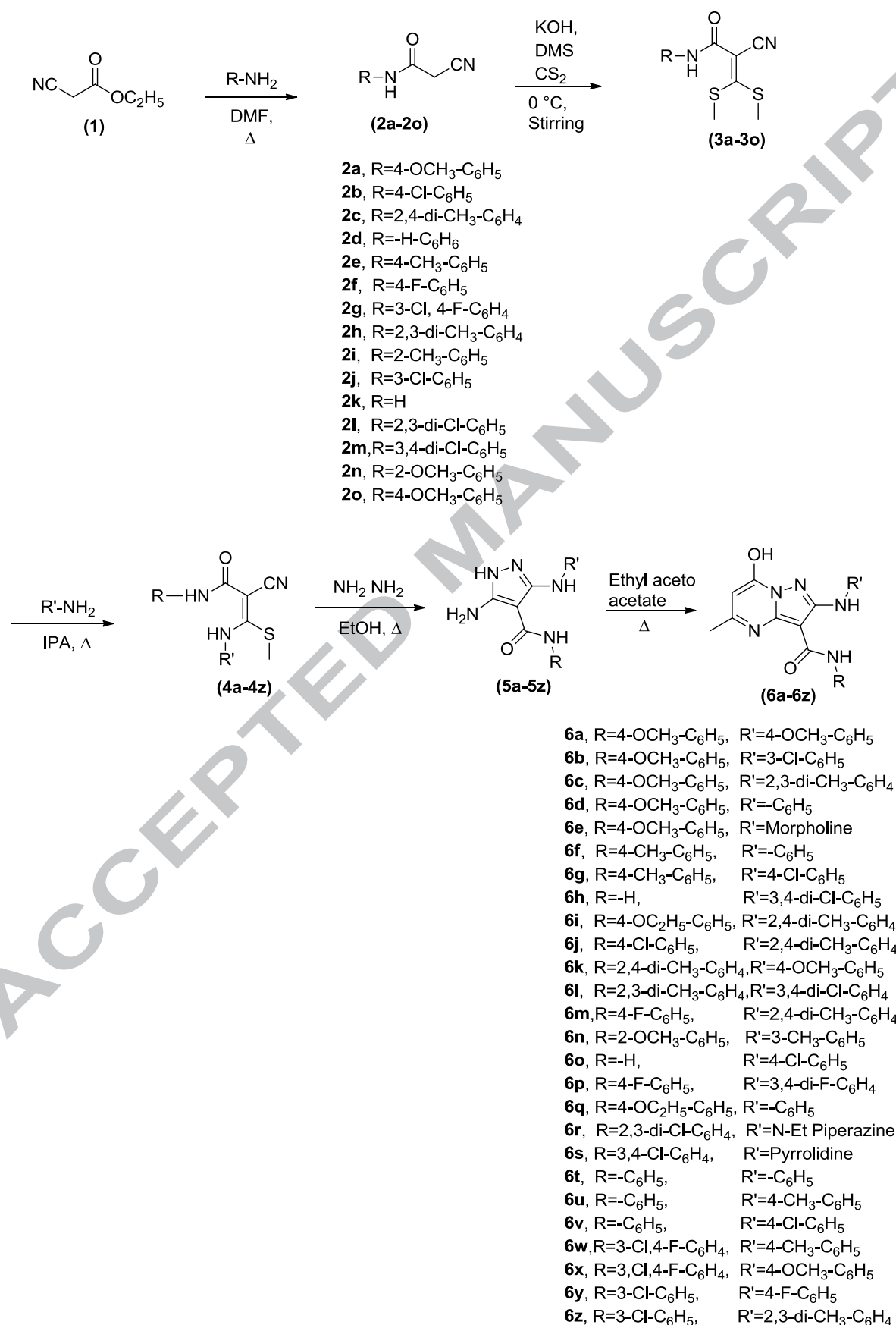


Table 1. ADMET properties of synthesized potent compounds from (6a-6z)

Co mp.	MW	Log P o/w	Log S	QPP Caco	Log BB	QPlog HERG	Metab	QPLog Khsa	% Oral abs
6g	407.11	4.145	-5.923	1247.131	-0.58	-6.453	6	0.458	100
6h	351.1	4.635	-6.45	1257.532	-0.68	-7.987	5	0.675	100
6n	403.4	4.67	-6.234	1104.734	-0.45	-6.128	6	0.483	100
6p	413.3	4.981	-6.542	1034.644	-0.65	-7.395	6	0.405	100

The acceptable molecular weight (MW) <500 Da; Predicted octanol/water partition coefficient (Log P) range is (2.0 to 6.5); Estimated solubility (Log S) should be greater than -4; QPPcaco 2 predicts gut-blood barrier in nm/s permeability of the cell model with ideal limit <25 (poor) and >500 (excellent); QPlogHERG used to identify the IC₅₀ value for blockage of HERG K⁺ channels range with range of >-5; metab predicts number of metabolic reactions with range of 1-8; binding to human serum albumin can be predicted through QPlogKhsa with range of -1.5 to 1.5; Human oral absorption in percentage predicts the oral human absorption with range of 0-100% scale.

Table 2. Anti-mycobacterial activity of pyrrazolo[1,5-*a*]pyrimidine (6a-6z)

Sample code	R	R'	MIC($\mu\text{g/ml}$)
6a	4-OCH ₃	4-OCH ₃	12.5
6b	4-OCH ₃	4-Cl	12.5
6c	4-OCH ₃	2,3-di-CH ₃	50
6d	4-OCH ₃	-NH	50
6e	4-OCH ₃	Morpholine	25
6f	4-CH ₃	-NH	50
6g	4-CH ₃	4-Cl	3.12
6h	-NH ₂	3,4-di-Cl	6.25
6i	4-Ethoxy aniline	2,4-di-CH ₃	50
6j	4-Cl	2,4-di-CH ₃	50
6k	2,4-di-CH ₃	4-OCH ₃	50
6l	2,3-di-CH ₃	3,4-di-Cl	50
6m	4-F	2,4-di-CH ₃	50
6n	2-OCH ₃	3-CH ₃	3.12
6o	-NH ₂	4-Cl	50
6p	4-F	3,4-di-F	0.8
6q	4-Ethoxy aniline	-NH	50
6r	2,3-di-Cl	N-Et piperazine	50
6s	3,4-di-Cl	Pyrrolidine	25
6t	-NH	-NH	50
6u	-NH	4-CH ₃	100
6v	-NH	4-Cl	50
6w	3-Cl 4-F	4-CH ₃	12.5
6x	3-Cl 4-F	4-OCH ₃	25
6y	3-Cl	4-F	12.5
6z	3-Cl	2,3-di-CH ₃	50
	Pyrazinamide		3.12
	Ciprofloxacin		3.12
	Streptomycin		6.25

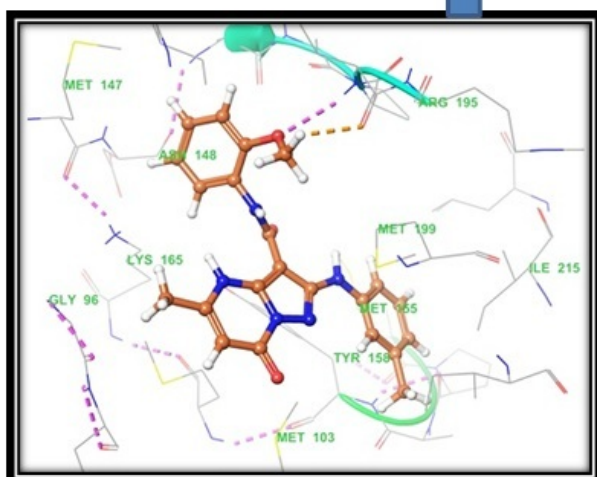
Table 3. MDR-TB and XDR-TB strain using Lowenstein-Jensen medium and Cytotoxicity study on Vero cell line

Sr. No.	R	R'	MIC ($\mu\text{g/mL}$)			Cytotoxicity IC ₅₀ ($\mu\text{g/mL}$)
			H37Rv	MDR-TB	XDR-TB	
6g	4-CH ₃	4-Cl	3.12	6.25	>100	20.99
6h	NH ₂	3,4-di-Cl	6.25	12.5	50	29.02
6n	2-OCH ₃	3-CH ₃	3.12	6.25	12.5	21.26
6p	4-F	3,4-di-F	0.8	3.12	25	13.57
	Isoniazid		0.5	6.25	50	ND

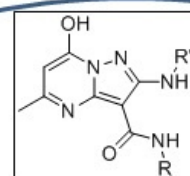
ND: Not determined

IC₅₀ values are the mean of triplicate study

SCRIPT



In-vitro anti-tubercular activity



		MIC
6p	R=4-F C ₆ H ₅ R'=3,4-F- C ₆ H ₄	0.8 µg/mL
6g	R=4-CH ₃ -C ₆ H ₅ R'=4-Cl- C ₆ H ₅	3.12 µg/mL
6n	R=2-OCH ₃ -C ₆ H ₅ R'=3-CH ₃ - C ₆ H ₅	3.12 µg/mL
6h	R=-H R'=3,4-Cl- C ₆ H ₄	6.25 µg/mL

ACCEPTED

Research highlight

- A series of pyrazolo[1,5-*a*]pyrimidine analogues were synthesized and screened for its anti-tubercular potential based on molecular docking study.
- Anti-tubercular potential was performed using Microplate Alamar Blue Assay (MABA) method for the preliminary screening against *Mycobacterium tuberculosis* H37Rv strain.
- Based on the preliminary screening Structure Activity Relationship (SAR) was generated.
- Compound **6g**, **6h**, **6n** and **6p** were found to be the most potent further opted for MDR-TB, XDR-TB and cytotoxicity study.